Title
EQUILIBRATION, COMPRESSION AND FLOW AT THE BEVALAC

Author
Pugh, H.G.

Publication Date
1984-07-01

LBL-18166

Lawrence Berkeley Laboratory
UNIVERSITY OF CALIFORNIA

Invited paper presented at the Fourth International Conference on Ultra-Relativistic Nucleus-Nucleus Collisions, Helsinki, Finland, June 17-21, 1984

EQUILIBRATION, COMPRESSION AND FLOW AT THE BEVALAC

H.G. Pugh

July 1984

NUCLEAR SCIENCE DIVISION

Prepared for the U.S. Department of Energy under Contract DE-AC03-76SF00098

DISCLAIMER

LBL-18166

EQUILIBRATION, COMPRESSION AND FLOW AT THE BEVALAC*

Howel G. Pugh
Nuclear Science Division
Lawrence Berkeley Laboratory
University of California
Berkeley, California 94720

Invited paper presented at the Fourth International Conference on Ultra-relativistic Nucleus-Nucleus Collisions, Helsinki, Finland, 17-21 June, 1984

---

*This work was supported by the Director, Office of Energy Research, Division of Nuclear Physics of the Office of High Energy and Nuclear Physics of the U.S. Department of Energy under Contract DE-AC03-76SF00098.

EQUILIBRATION, COMPRESSION AND FLOW AT THE BEVALAC*

Howel G. Pugh
Nuclear Science Division
Lawrence Berkeley Laboratory
University of California
Berkeley, California 94720

This paper presents data acquired in the past two years by the Streamer Chamber group1) and the Plastic Ball group.2) I shall present evidence that at Bevalac energies, head-on nuclear collisions result in stopping; I shall present evidence for collective flow of the interacting nuclei; I shall present evidence that a substantial part of the energy is tied up in compressional energy at the high density phase of the collision; finally, I shall present recent data concerning aspects of the collisions such as interaction volume, particle ratios and temperatures. At the meeting at Bielefeld two years ago, it was not possible3) to make definitive statements about most of these subjects: the progress in the intervening period has been remarkable.

1. ^{40}Ar + Pb Central Collisions at 0.77 AGeV

Central collisions can be selected by placing a detector of suitable size at 0° and requiring that no projectile fragments are observed in that detector, i.e., the target nucleus completely overlapped the projectile (as seen along the beam direction). For equal mass nuclei this indicates the impact parameter $b = 0$; for a light projectile on a heavy target it indicates $b < r_{target} - r_{projectile}$. The cascade model shows that the participant proton multiplicity M_p can also be used as an approximate measure of impact parameter.

This method has been used to study ^{40}Ar + Pb central collisions at 0.77 AGeV, using the LBL Streamer Chamber facility.4,5) Figure 1 shows the distribution of participant proton multiplicity M_p, as well as a comparison with the results of an intranuclear cascade calculation.6) We shall later divide the data into two groups: high M_p and low M_p corresponding to $b < 3$ fm and 3 fm $< b < 5.5$ fm respectively.

To test for stopping, the simplest test is for isotropy in the c.m. system of the participant protons, taken on an event-by-event

---

*This work was supported by the Director, Office of Energy Research, Division of Nuclear Physics of the Office of High Energy and Nuclear Physics of the U.S. Department of Energy under Contract DE-AC03-76SF00098.

basis. This requires the quantity R, defined by R = $\frac{2}{\pi} \sum_{\nu=1}^{N} |P_\perp|_\nu \Big/ \sum_{\nu=1}^{N} |P_\parallel|_\nu$ to equal unity, where the sums are taken over the number of protons observed in each event. Figure 2 shows a contour diagram of R versus M_p. It is seen that for the lower M_p (larger impact parameters) R is less than unity, indicating incomplete equilibration. However as M_p increases, R crosses unity at about M_p = 40 and even exceeds unity, suggesting some kind of side splash. On the other hand, the cascade model predictions only approach unity so that the nuclei seem to be somewhat more efficient in stopping each other than expected in that model. Figure 3 shows a contour diagram of $\frac{2}{\pi} \langle P_\perp \rangle$ versus $\langle P_\parallel \rangle$ for the high M_p cut. The dashed line indicates R = 1.

It is interesting to look beyond this at the event shapes, for which it is convenient first to identify the reaction plane for each event. This is the plane containing the beam direction such that the summed projection of momenta perpendicular to the plane is zero. All events can be rotated into the same reaction plane; no physics is lost by this process, for unpolarized beam and target. Figure 4 shows a contour diagram of proton transverse and longitudinal momenta in the reaction plane for the low M_p cut, 3 fm < b < 5.5 fm (the cut shows the region of detector inefficiency near the target). A systematic event shape is seen, showing an average sideways deflection of the participants. It is remarkable that the events show symmetry about the origin even though there is a different number of participants from the two interacting nuclei.

2. Flow Tensor Analysis and Collective Flow

To characterize the shape in momentum space of each event some further parameterization is necessary. One method is to introduce the flow tensor $T_{ij} = \sum_{\nu=1}^{N} P_{i\nu} P_{j\nu} \omega(\nu)$ where the sum is over all the particles in a given event, i,j, and k are the cartesian coordinates, and ω is a weighting factor. The weighting factor has recently been taken as $\omega_\nu = 1 \Big/ |P_\nu| \sum_{\nu=1}^{N} |P_\nu|$ in the streamer chamber data, so that T represents momentum flow. The plastic ball group has preferred $\omega_\nu = 1/2m_\nu$, yielding energy flow. The results are insensitive to the choice of weighting, which adds confidence that the conclusions are significant.

Such an analysis yields six quantitities characterizing the flow tensor: The lengths of the three axes of an ellipsoid, and three orientation angles. This is a great number of parameters to fit even to the large amount of data obtained, and we restrict ourselves here to the "flow angle," i.e. the value of θ for the longest axis of the ellipsoid, measured relative to the beam direction. Figure 5 shows data obtained by the Plastic Ball group[7)] for ^{40}Ca + Ca and ^{93}Nb + ^{93}Nb at 0.4 AGeV. The data for ^{93}Nb show a well-developed peak in the flow angle which increases in angle as the charged particle multiplicity increases, i.e. as the impact parameter decreases. The effect, while present in the ^{40}Ca data, is less clear, demonstrating the value of using heavy nuclei for these studies. Calculations using a cascade code[8)] do not show the effect, suggesting that collective phenomena are being observed.[9)] Figure 6 shows results similar to those of Figure 4, but taken with the Plastic Ball. Note that the experimental data, which should be symmetric between target and projectile, show detector inefficiencies in the backward hemisphere; these have been taken into account in applying the cascade predictions.

That these results provide evidence for relativistic hydrodynamics is shown by calculations by Buchwald et al.[10)] whose results are shown in Figure 7. They are in qualitative agreement with the data. However, it is very difficult to introduce individual particle effects such as detector inefficiencies into hydrodynamic calculations, and much work remains to be done. New data on ^{139}La + ^{139}La and ^{197}Au + ^{197}Au will be available soon.

In addition to the flow angle, the shapes of the momentum (or energy) ellipsoids are of interest. In general events seem to be prolate, with the longest axis closest to the beam direction. However, for b = 0 collisions of equal mass nuclei, one might expect an oblate spheroid with its shortest axis along the beam direction, and a flow angle of 90°. This would also give a value greater than unity for the R ratio discussed earlier. The data presented in Figure 5 do not approach b = 0 for ^{93}Nb + ^{93}Nb since the charged multiplicity for such events should be about 80. While the situation is not quite analogous, it is therefore necessary to return to the ^{40}Ar + Pb data at 0.77 GeV/n. Here since the radii of ^{40}Ar + ^{208}Pb are roughly 4 fm and 7 fm respectively, the higher multiplicity sample, $b < 3$ fm, corresponds to complete overlap of the two nuclei while the lower multiplicity sample, 3 fm $< b <$ 5.5 fm, is closer to the nuclear peripheries. Figure 8(a) shows the flow angle distributions for the two multiplicity cuts. The low M_p sample shows a flow pattern similar to that seen in Figure 5 for Nb + Nb, which seems to be characteristic of intermediate impact parameters for heavier nuclei. The high

M_p sample is roughly isotropic, while the event shapes are approximately spherical. Thus the anticipated oblate event shape is approached but not definitely observed. Figure 8(b) shows intranuclear cascade calculations$^{6,9)}$ for the same impact parameter cuts. No collective flow effect comparable to those seen in the data is observed.

3. Collective Effects in the Energy

A detailed analysis of the final state energy shows, for both streamer chamber and plastic ball data, that all the initial energy is accounted for. What would be interesting is a breakdown of the total energy into collective and random components as a function of time during the collision. In the initial state all the energy is collective. An analysis of the plastic ball data on Nb + Nb$^{7)}$ shows that roughly 10% of the energy in the final state appears in non-isotropic components of the collective flow. Extraction of the radial component is difficult because it can be confused in the data with the thermal component,$^{11)}$ and its extraction involves a very detailed analysis of the energy spectra.

An estimate of the energy tied up in compression at the maximum-density phase of the collision has been given by Stock, Harris et al.$^{12,13)}$ They used the streamer chamber to study ^{40}Ar + KCl as a function of energy. At each energy the π^- yield was measured as a function of proton participant number and extrapolated to $b = 0$, as shown in Figure 9. The results shown in Figure 10 as a function of energy indicate as a function of energy a substantial reduction below the predictions either of cascade calculations or of a chemical model, though the theories agree with each other. The interpretation offered is simple: at each beam energy, if the energy available for pion production is reduced by the amount shown by the horizontal arrows in Figure 10 the correct number of pions would be obtained. The deficiency is attributed to energy required to compress the nuclear matter, which is not allowed for in the theoretical results. Since the theories provide the density reached in the collision it is possible to go one step further and derive an equation of state for nuclear matter, as shown in Figure 11. Despite criticism of the procedure in detail, the concept has not been invalidated and it remains as the only means so far of extracting an equation of state from experimental data.

Overall, we thus have a rough idea of how the energy is degraded during the collision, if we are willing to mix results from such disparate experiments as Nb + Nb at 0.4 AGeV and Ar + KCl at 0.5 - 1.8 AGeV. At maximum density, where there can be no flow effects, about 35% of the energy seems to be tied up in compression while 65% must have gone into thermal motion, including pion creation. In the final state, 10% of the energy has been identified in non-radial flow. It would be very valuable to complete this picture.

4. Other New Plastic Ball Data

A high-statistics study of two-proton intensity interferometry has been made for ^{40}Ca + Ca and ^{93}Nb + ^{93}Nb at 0.4 AGeV.[14)] Figure 12 shows a fit which includes the effects of Coulomb repulsion, final-state interaction and experimental resolution. Figure 13 shows the systematic behavior of the extracted radius parameter as a function of participant number, defined as $N_p A/Z$ where N_p is the measured number of protons. The fits shown use the formula

$$r = r_o \, (N_p A/Z)^{1/3} / \sqrt{5/2}$$

The factor of $\sqrt{5/2}$ is to convert the radius from a hard-sphere to a gaussian. The proportionality to the cube root of the participant number is presumably an approximation since the emitting volume is hardly likely to be spherical at all impact parameters. Nevertheless the result is extremely suggestive, because the hard sphere radius constant extracted is $r_o = 1.9$ fm, corresponding to freeze-out at about 25% of nuclear density. The protons appear therefore to be emitted at a very late stage of the reaction.

Some supporting evidence is given by observations of deuteron-proton ratios,[15)] shown in Figure 14. The d/p ratio increases with multiplicity, and can be explained if the participant volume increases as $(N_p A/Z)^{1/3}$, as before. The freeze-out here occurs at about 50% of nuclear density.

A possibly related result appears in other data from the same reactions. The proton energy spectra were fitted with Boltzmann distributions and "temperatures" extracted, as a function of charged multiplicity. The results,[16)] given in Table 1, show that the temperature is an increasing function of multiplicity. While the numbers have not been explained qualitatively, the authors suggest that the rise may be due to the increasing d/p ratio: when a neutron and proton coalesce to form a deuteron, the number of degrees of freedom diminishes, which increases the temperature (the energy release in the process $n + p \rightarrow d$ is negligible).

Table 1
Temperature as a function of multiplicity[15)]
(Plastic Ball--0.4 AGeV)

charged multiplicity		0-10	10-20	20-30	30-40	40-50	50-60
T(MeV)	Ca + Ca	43	48	54	56		
	Nb + Nb	42	46	51	55	60	65

5. Some New Results from the Streamer Chamber on Pion Spectra

An analysis has recently been completed of pion and proton spectra in central ^{40}Ar + KCl collisions at 1.8 GeV/n.[17)] The conclusions are as follows:

a) 85% of the pions are emitted isotropically.

b) The remaining anisotropy can be attributed to the "corona effect" observed in equal-mass collisions.

c) The pion spectra can be fitted fairly well with intranuclear cascade calculations, except for a 5% high temperature component.

d) The predominant pion temperature is 58 MeV compared with 118 MeV for the protons and 111 MeV for the 5% pion component.

e) At first sight this is a disaster for any thermodynamic ideas of equilibrium, but once the kinematics of Δ decay are introduced, everything falls into place. The cascade calculations[4)] already include the kinematics, and if the source of pions and protons is assumed to be the decay of Δ's in equilibrium with the protons, the thermodynamic model is also reconciled with the data.

f) However, it is not possible on the basis of the present data, and it will always be difficult, to separate the effects of radial flow.[11)] Whether the Δ temperature is a true temperature or an effective temperature made by folding a lower true temperature with radial flow makes little difference to the final pion and proton spectra.

6. Conclusions

The amount of data growing out of the Bevalac is qualitatively greater than a few years ago, and we look forward to significant progress in understanding in the next few years also.

Acknowledgments

I am grateful to the members of the Streamer Chamber and Plastic Ball collaborations[1,2)] for helping me assemble this paper, and to the Organizers of this Conference for asking me to present it.

This work was supported by the Director, Office of Energy

Research, Division of Nuclear Physics of the Office of High Energy and Nuclear Physics of the U.S. Department of Energy under Contract DE-AC03-76SF00098.

References

1. D. Bangert and W. Rauch, Univ. of Marburg; R. Bock, R. Brockmann, J.W. Harris, M. Maier, A. Sandoval, R. Stock, and H. Strobele, GSI; A.Dacal and M.-E. Ortiz, UNAM, Mexico; G. Odyniec, H.G. Pugh, and L.S. Schroeder, LBL; R.E. Renfordt, D.Schall, and K. Tittel, Univ. of Heidelberg; K.W. Wolf, Texas A M University.

2. H.-A. Gustafsson, M. Doss, A.M. Poskanzer, T. Renner, H. Riedesel, and A. Warwick, LBL; H.H. Gutbrod, B. Kolb, H.-G. Ritter, F. Weik, and H. Wieman, GSI; K.-H. Kampert and H. Lohner, Univ. of Munster; B. Ludewigt, Univ. of Marburg.

3. H.G. Pugh, (Bielefeld Workshop on) Quark Matter Formation and Heavy Ion Collisions, ed. M. Jacob and H. Satz, World Scientific (1982), p. 185

4. H. Stroebele et al., Phys. Rev. C27, 1349 (1983); note that for ^{40}Ar + Pb the c.m. frame of the participant protons has been extracted on an event-by-event basis by using the measured momenta.

5. R.E. Renfordt et al., Phys. Rev. Lett. 53, 763 (1984).

6. J. Cugnon, T. Mitzutani, and J. Vandermeulen, Nucl. Phys. A352 505 (1981);
   J. Cugnon, D. Kinet, and J. Vandermeulen, Nucl. Phys. A379, 553 (1982)

7. H.A. Gustafsson et al., Phys. Rev. Lett. 52, 1590 (1984)

8. Y. Yariv and Z. Fraenkel, Phys. Rev. C20, 227 (1979)

9. The paper presented by Cugnon at this conference suggests that the flow effect is present in cascade calculations. However, it is interesting to note that the calculations used for comparison with the streamer chamber data for ^{40}Ar + Pb (presented later in the present paper) used Cugnon's code, and showed no flow.

10. G. Buchwald et al., Phys. Rev. Lett. 52, 1594 (1984)

11. P. Siemens and J. Rasmussen, Phys. Rev. Lett. 42, 880 (1979)

12. R. Stock et al., Phys. Rev. Lett. 49 (1982) 1236

13. J.W. Harris et al., LBL-17404 (1984), to be published.

14. H.-A. Gustafsson et al., Phys. Rev. Lett. 53, 544 (1984).

15. H.H. Gutbrod et al., Phys. Lett. 127B, 317 (1983)

16. H.-A. Gustafsson et al., GSI-84-9 (1984), and to be published.

17. R. Brockmann et al., LBL-17755 (1984), to be published.

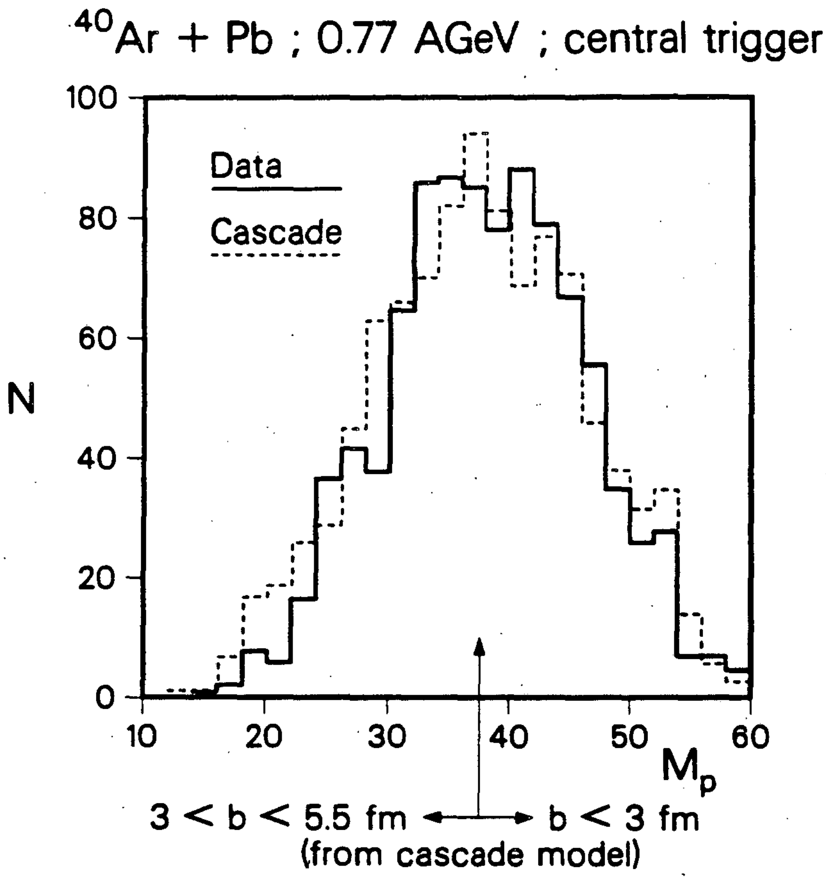

Figure 1

Multiplicity distribution of participant protons and comparison with cascade model predictions.

XCG 848-13227

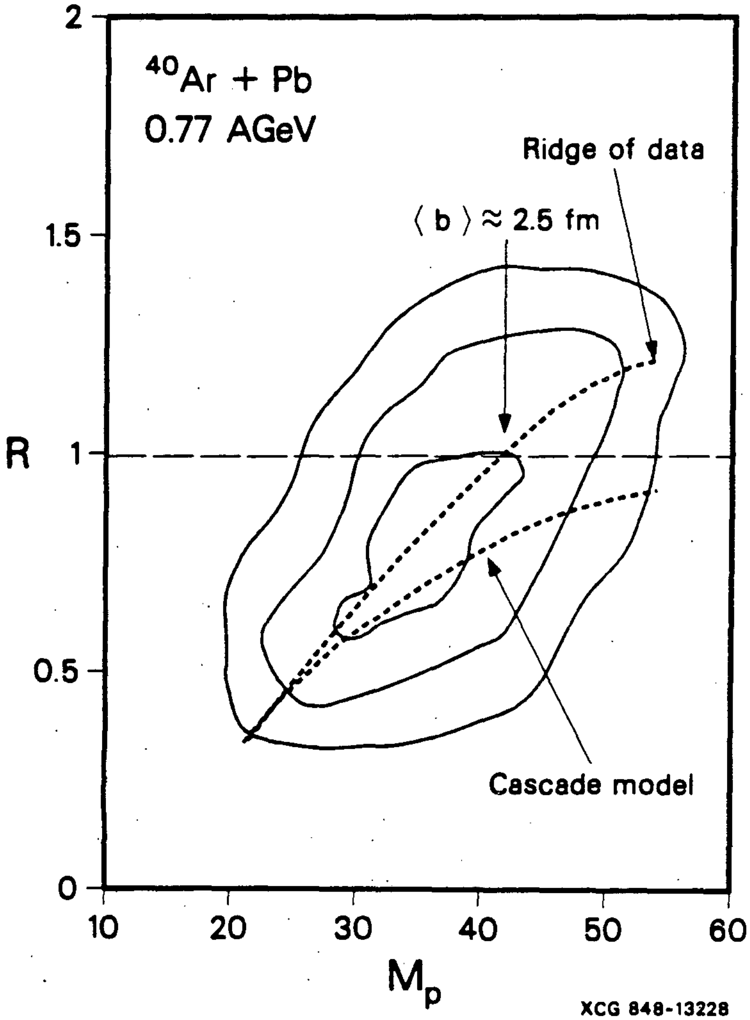

Figure 2

Contour plot of the ratio R versus the participant proton multiplicity. The ratio R should equal unity if equipartition occurs.

XCG 848-13228

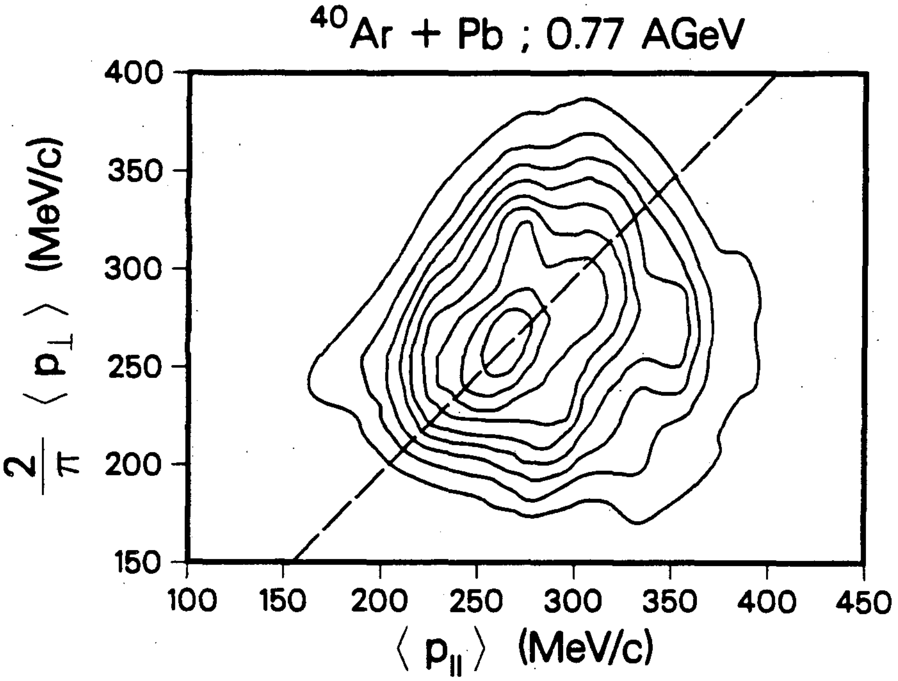

XCG 848-13229

Figure 3

Contour plot of $\frac{2}{\pi}$ $<p_\perp>$ versus $<p_\|>$. The line shows the expected locus for complete equipartition.

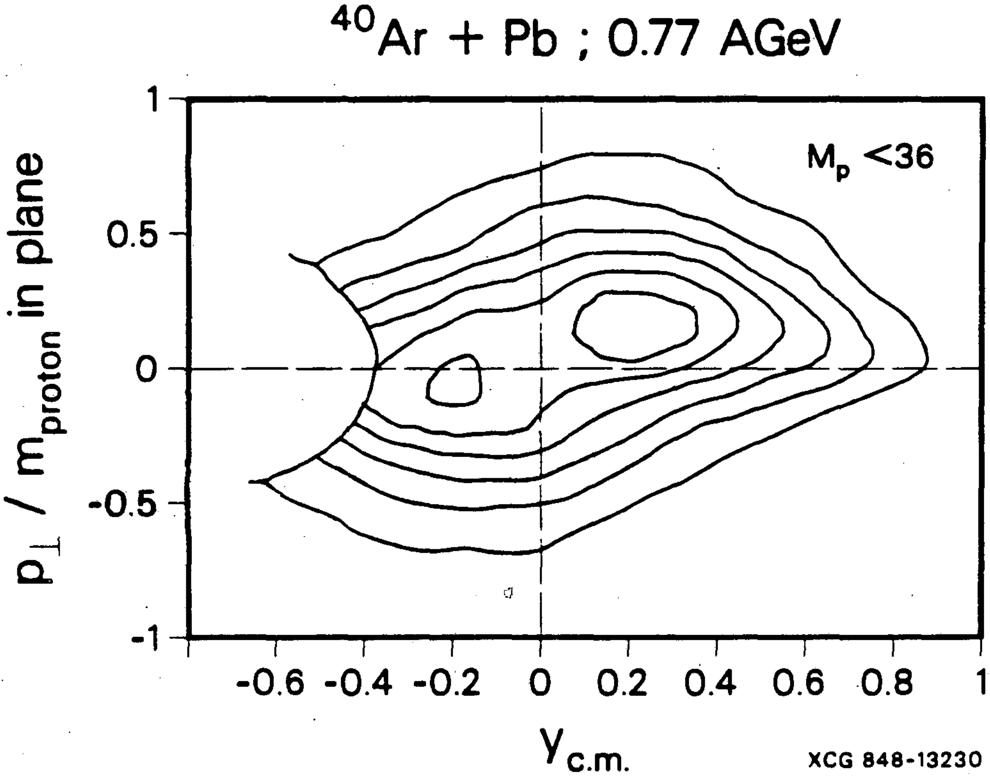

XCG 848-13230

Figure 4

Contour plot of $p_\perp/m_p$ versus y_{cm}, after all events have been rotated so that the reaction planes coincide. Streamer Chamber data.

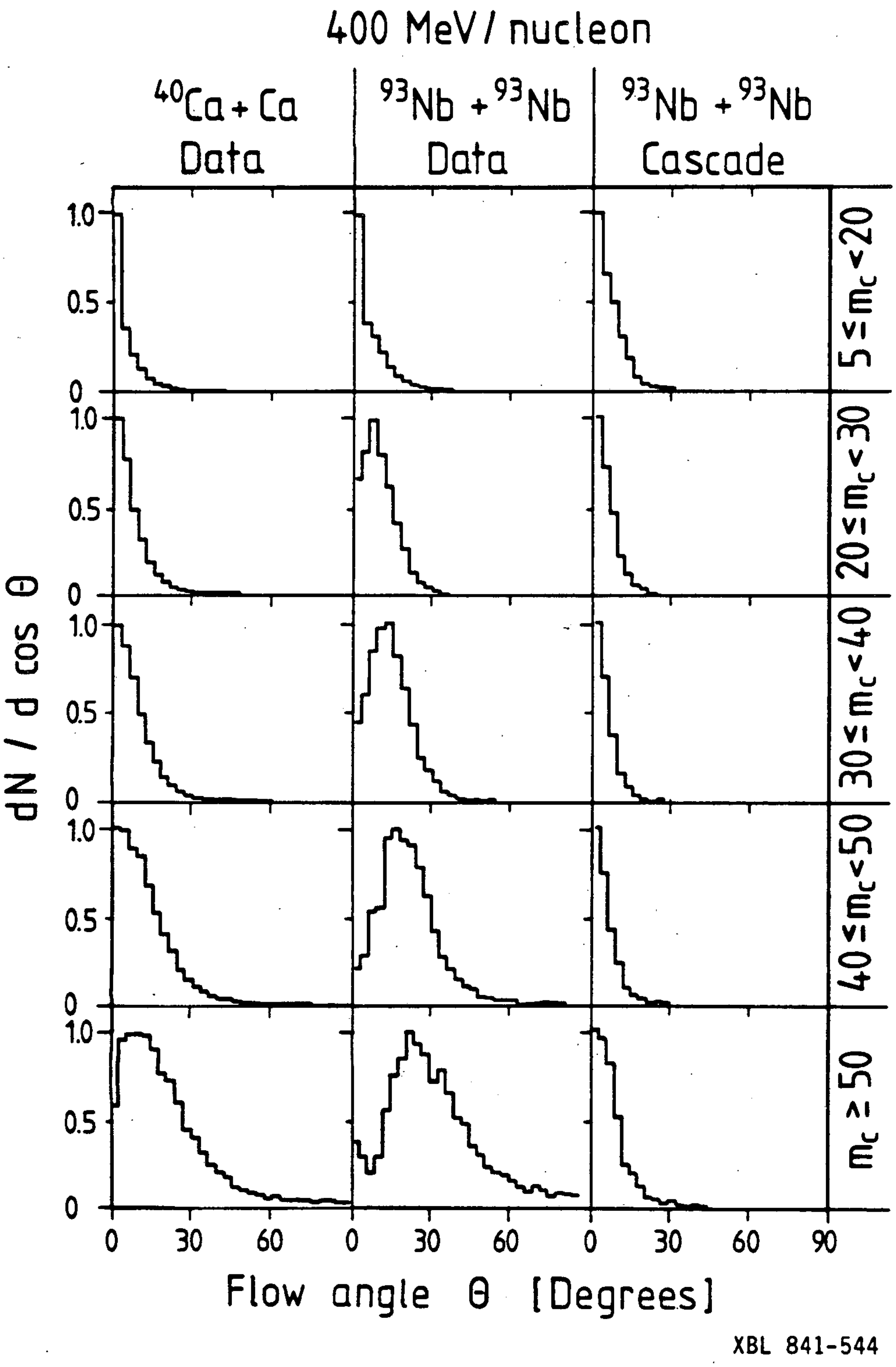

Figure 5

Flow angle distributions for Ca + Ca and Nb + Nb collisions and cascade predictions for Nb + Nb. Plastic Ball data.

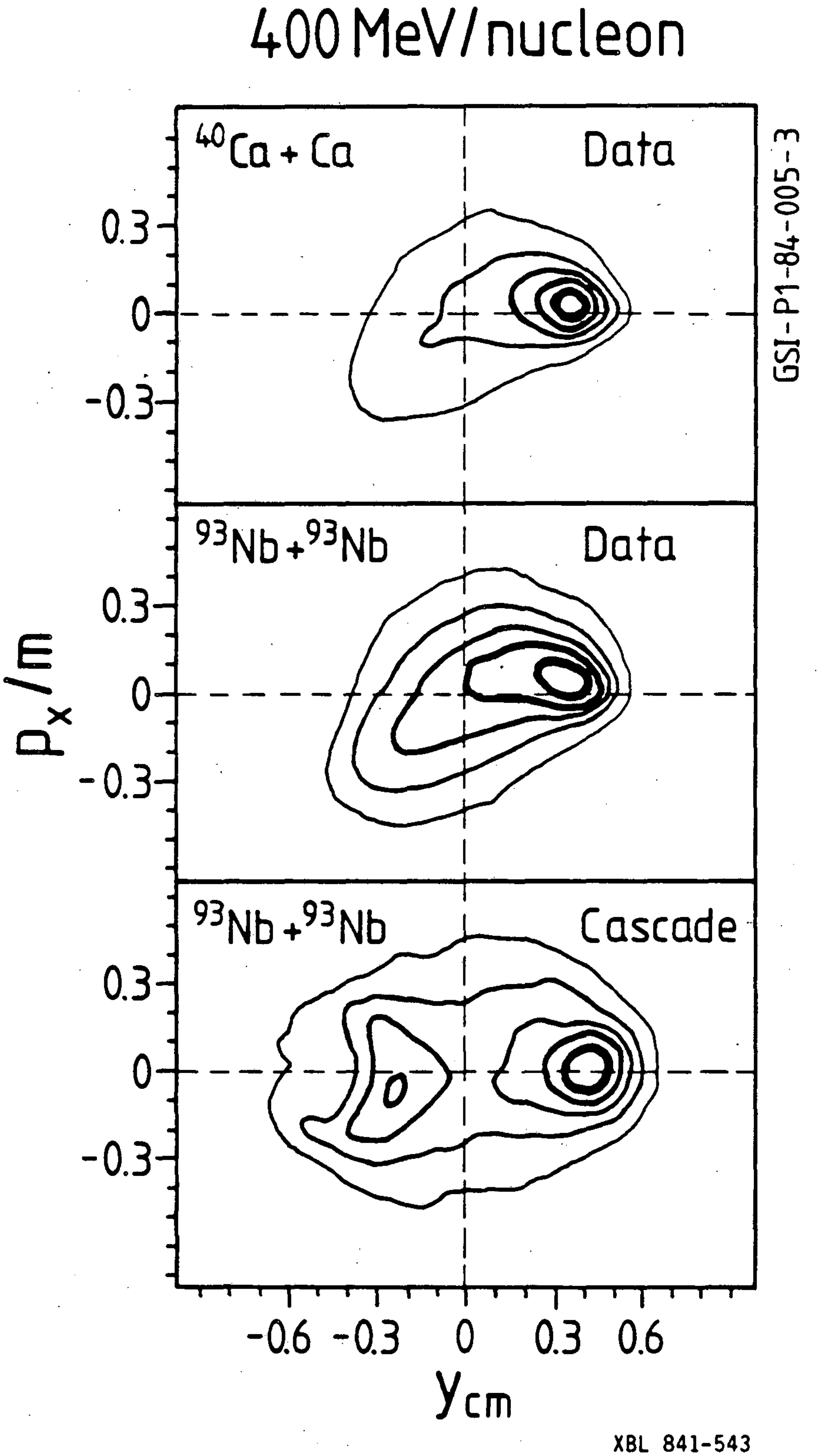

XBL 841-543

Figure 6

Contour plots of P_x/m versus y_{cm} after all events have been rotated so that their reaction planes coincide. Plastic Ball data.

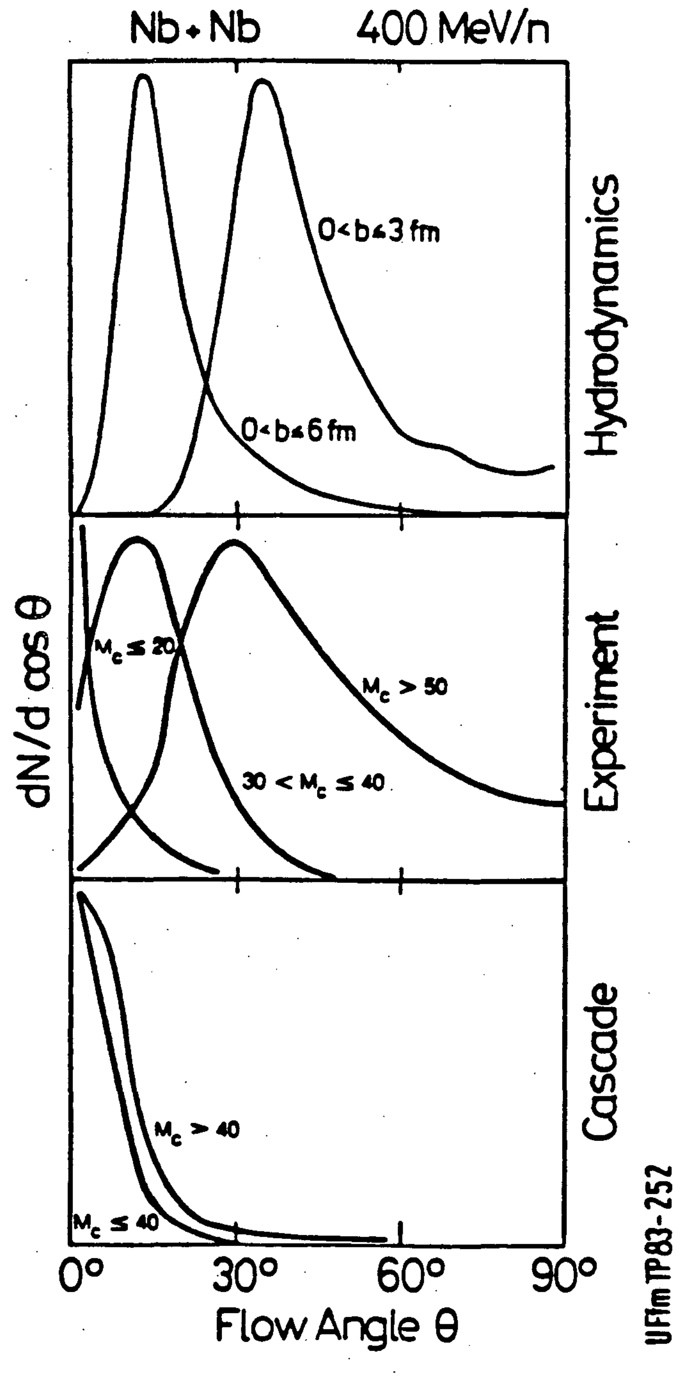

XBL 849-3692

Figure 7

Predictions of flow angle distributions derived from a relativistic hydrodynamic model.

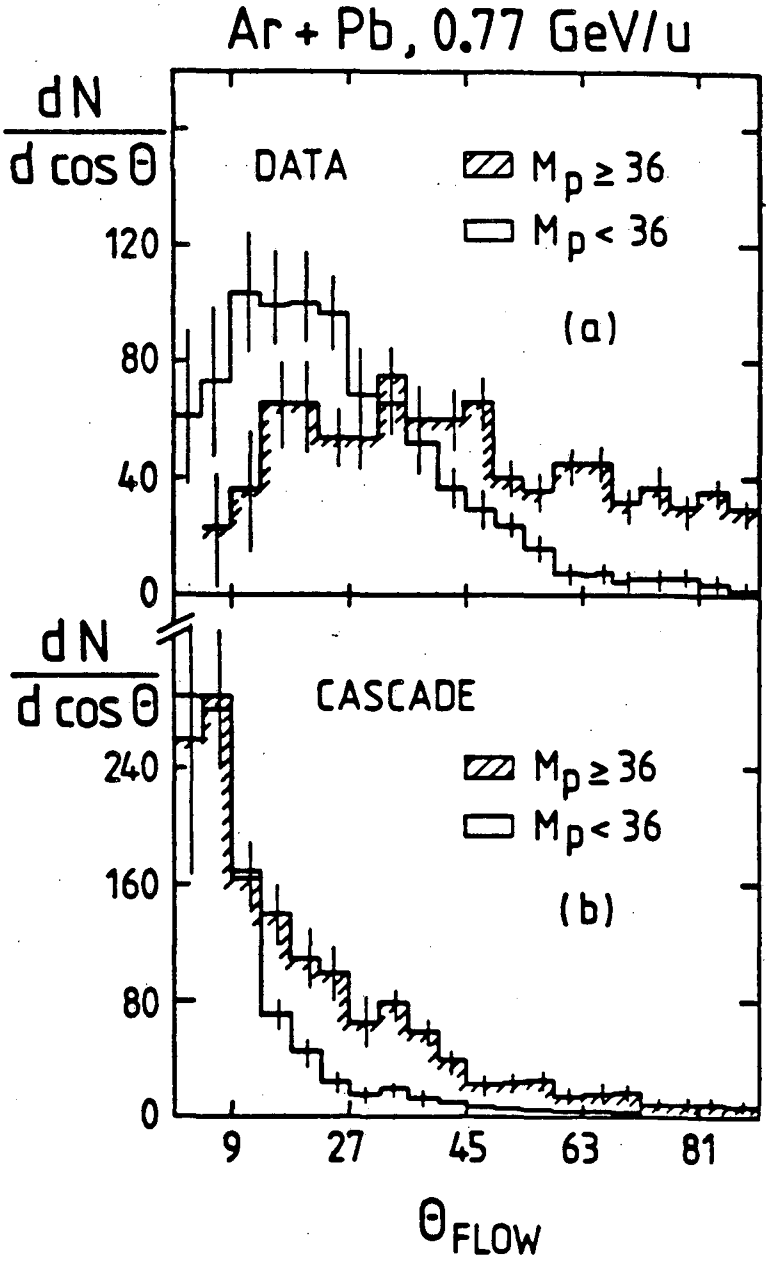

XBL 849-3693

Figure 8

(a) Flow angle distributions for two participant proton multiplicity samples corresponding to $b < 3$ fm ($M_p \geq 36$) and $3 < b < 5.5$ fm ($M_p < 36$). Streamer Chamber data.

(b) Corresponding predictions of the cascade model, corrected for detector acceptance.

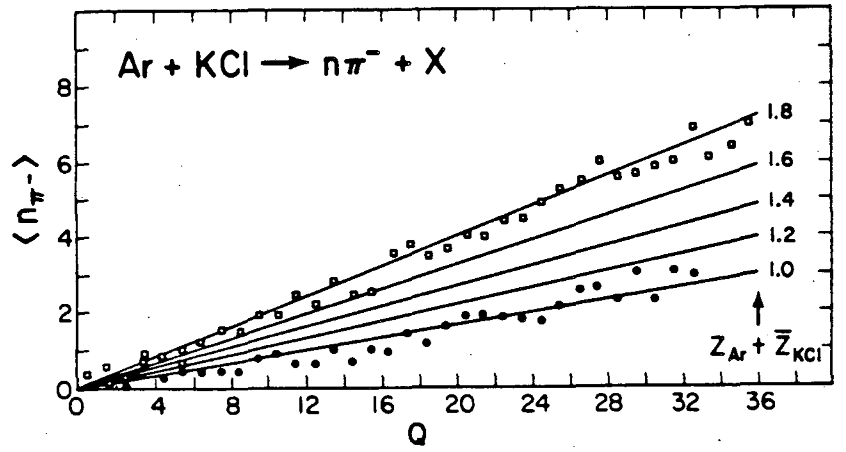

XBL804-747B

Figure 9

Multiplicity of π^- production versus participant proton multiplicity for various bombarding energies. The value extrapolated to $Z_{Ar} + Z_{KCl}$ corresponds to b = 0.

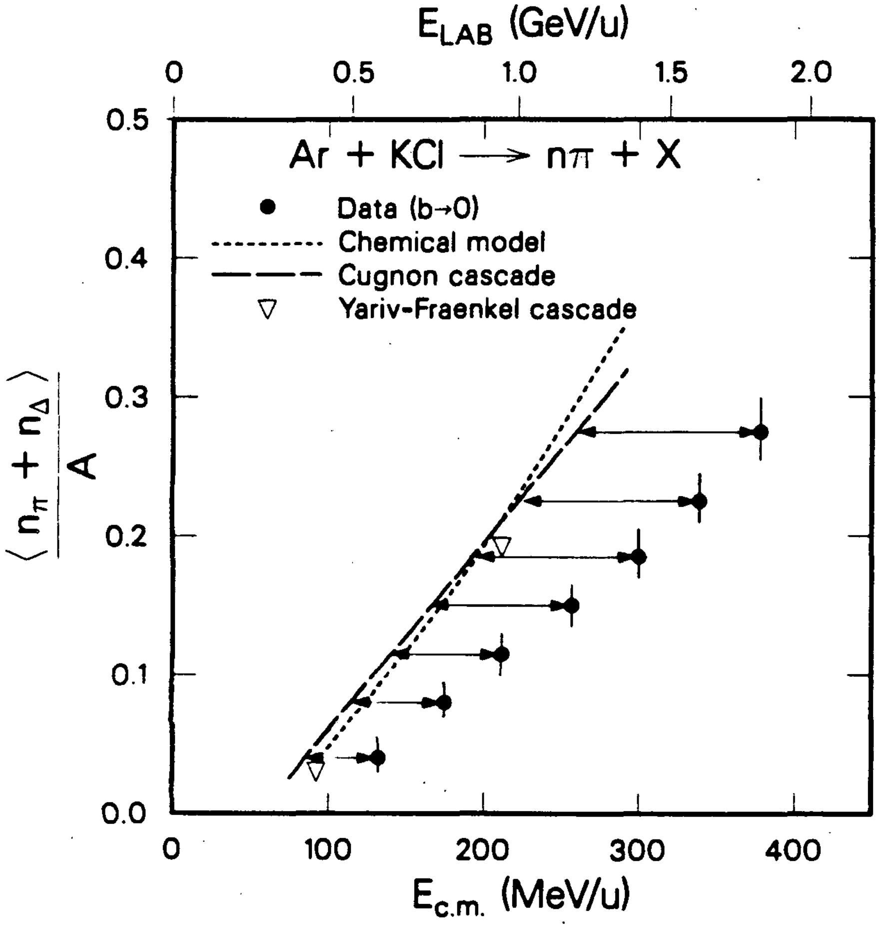

Figure 10

XCG 8312-4933

Pion multiplicities versus E_{cm} for Ar + KCl central collisions. The length of the arrows is assumed to reflect compressional energy.

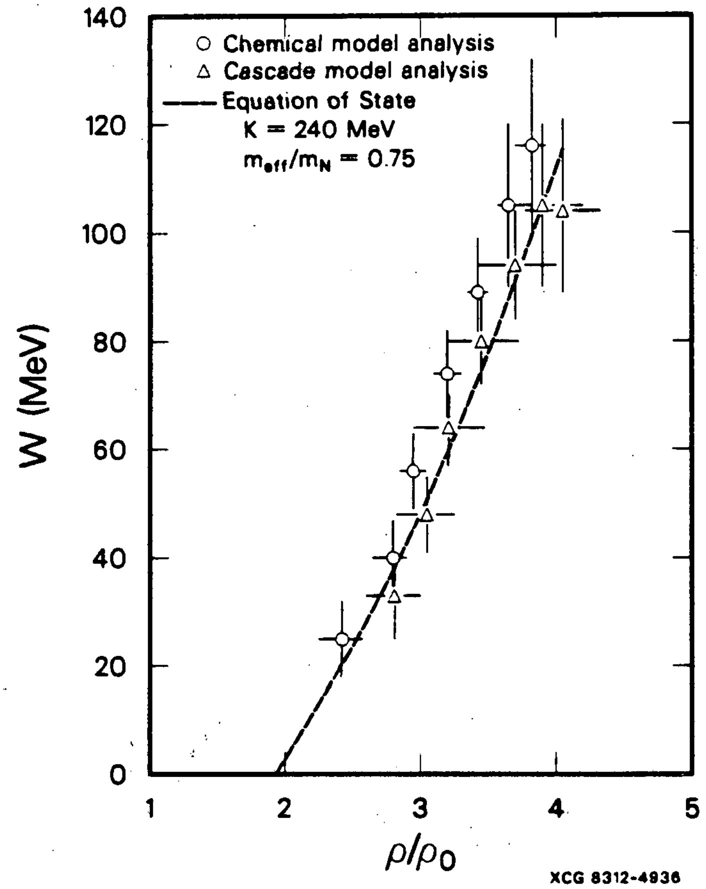

Figure 11

Equation of State derived from Figure 10. W is the compressional energy.

Figure 12

Two proton intensity interferometry data showing a theoretical fit. Plastic Ball data.

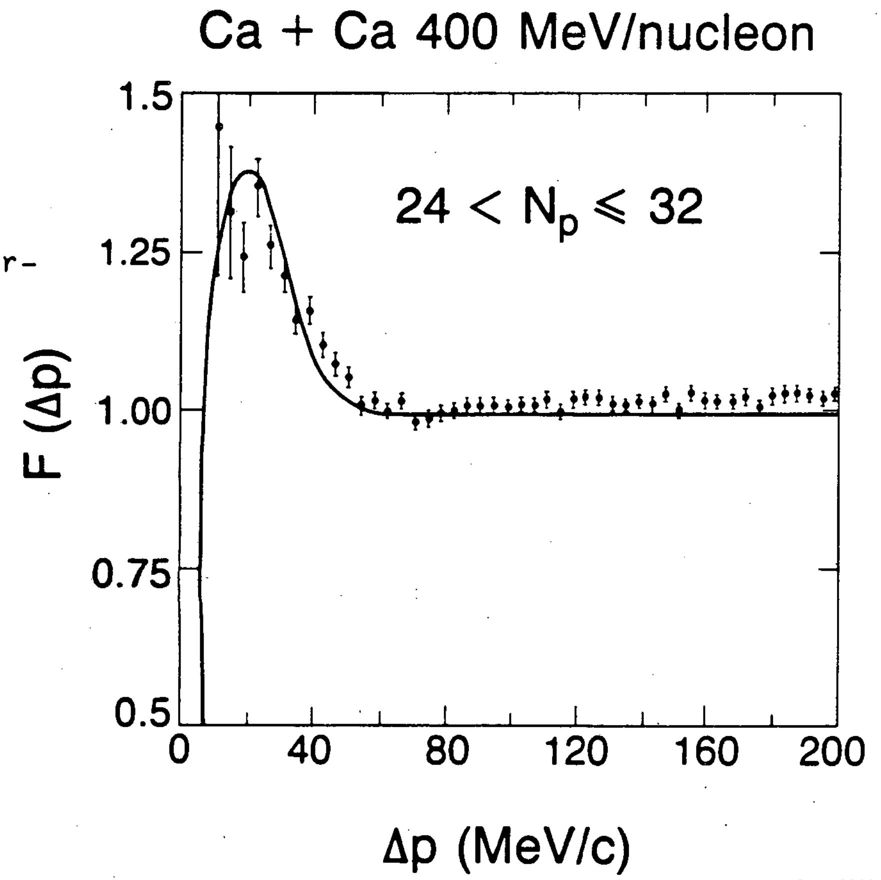

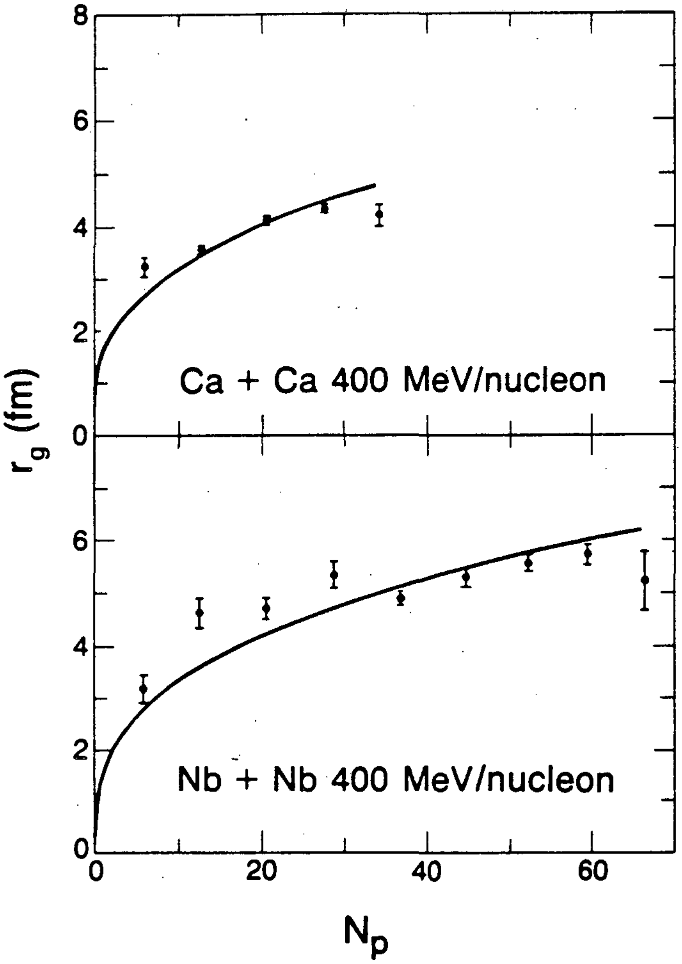

XBL 842-10058

Figure 13

Dependence of radius parameter extracted from two-proton intensity interferometry on the participant proton multiplicity. The curves correspond to ρ/ρ ~ 0.25.

Figure 14

The d (like)/p (like) rates extracted from Plastic Ball data. The curve corresponds to ρ/ρ_0 ~ 0.5.

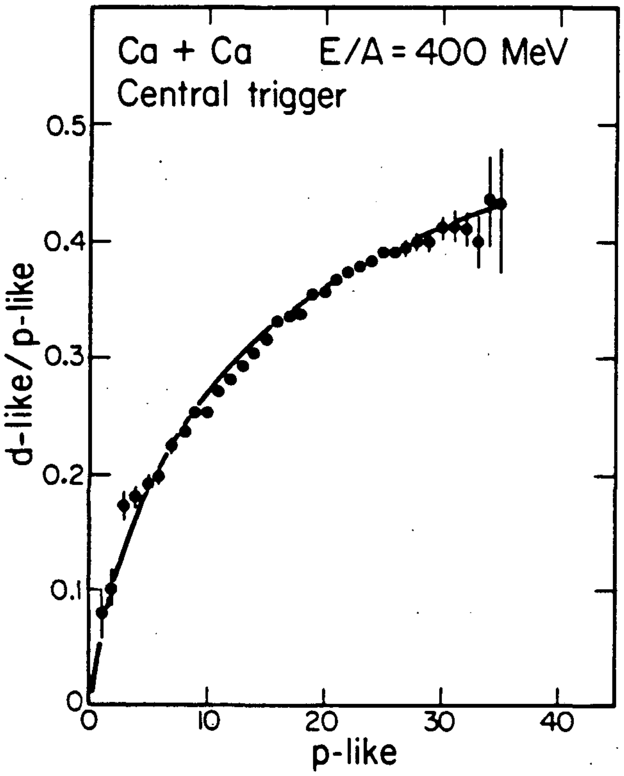

XBL 829 – 1162

TECHNICAL INFORMATION DEPARTMENT
LAWRENCE BERKELEY LABORATORY
UNIVERSITY OF CALIFORNIA
BERKELEY, CALIFORNIA 94720